



Synthesis and structural characterization of metal halide complexes containing *N,N'*-di(2-methoxyphenyl)formamidine (*o*-HDMophF)

Chun-Wei Yeh ^a, Hui-Ling Hu ^b, Rung-Hua Liang ^a, Kai-Ming Wang ^a, Ting-Yi Yen ^a,
Jhy-Der Chen ^{a,*}, Ju-Chun Wang ^c

^a Department of Chemistry, Chung-Yuan Christian University, No. 22 Pu Ren, Chung-Li, Taiwan 320, Taiwan, ROC

^b Department of Chemical Engineering, Nanya Institute of Technology, Chung-Li, Taiwan, ROC

^c Department of Chemistry, Soochow University, Taipei, Taiwan, ROC

Received 5 June 2004; accepted 14 December 2004

Abstract

The reactions of *N,N'*-di(2-methoxyphenyl)formamidine (*o*-HDMophF) with transition metal halide complexes afforded $\text{CuCl}_2 \cdot (\textit{o}\text{-HDMophF})$, **1**, $[\text{CoX}_4][\textit{o}\text{-H}_2\text{DMophF}]_2$ ($\text{X} = \text{Cl}$, **2**; Br , **3**) and $\text{MCl}_2(\textit{o}\text{-HDMophF})_2$ ($\text{M} = \text{Cd}$, **4**; Ni , **5**; Mn , **6**; Pd , **7**). These complexes were characterized by single-crystal X-ray diffraction and elemental analyses. The neutral *o*-HDMophF ligands in complexes **4–6** and **7** are coordinated to the metal centers in new bidentate and monodentate fashions, respectively. In the crystal structures of **1–7**, C–H...X and/or N–H...X ($\text{X} = \text{Cl}$, Br) interactions are found to link the metal units to the *o*-HDMophF ligand or its protonated cation ($\textit{o}\text{-H}_2\text{DMophF}^+$). The neutral *o*-HDMophF compound in **1** adopts the *s-trans-anti-s-trans*-conformation, while those in complexes **4–6** and **7** adopt the *s-trans-anti-s-trans*- and *s-cis-anti-s-trans*-conformations, respectively. The $\textit{o}\text{-H}_2\text{DMophF}^+$ cations of complexes **2** and **3** adopt the *s-cis-syn-anti-s-trans* and *s-trans-anti-anti-s-trans* conformations. © 2005 Elsevier Ltd. All rights reserved.

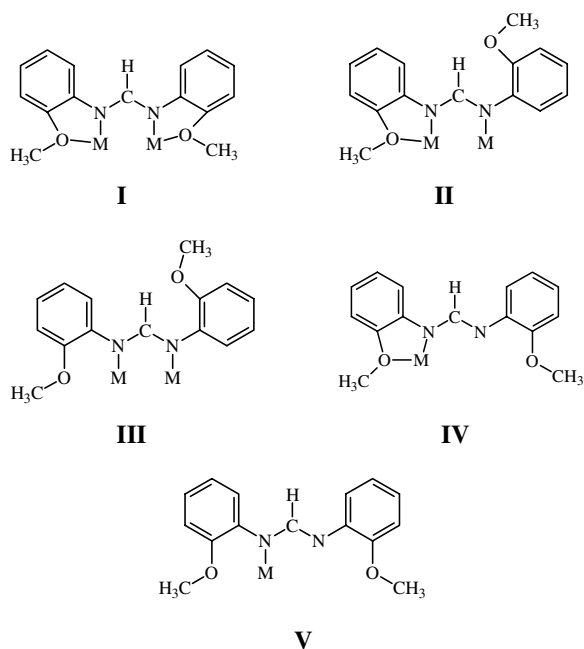
Keywords: Metal halide complexes; Conformation; X-ray structure; Hydrogen bonds; *N,N'*-Di(2-methoxyphenyl)formamidine

1. Introduction

The anion of the compound *N,N'*-di(2-methoxyphenyl)formamidine, *o*-DMophF[−], has been subjected to several studies of its coordination ability to metal centers. Tetradentate, tridentate and bidentate coordination modes **I–III** (Scheme 1) have been seen for this anion. In the tetradentate mode of coordination, **I**, two nitrogen atoms and two oxygen atoms are chelating and bridging to the metal centres. Such coordination was found in the dinuclear complex $\text{Ag}_2(\textit{o}\text{-DMophF})_2$ [1]. The coordination mode, **II**, which features chelation by one nitrogen

atom and one oxygen atom together with the formation of a bridge through the two nitrogen atoms, was found in the dinuclear complex *trans*- $\text{Ru}_2(\text{O}_2\text{CCH}_3)_2(\textit{o}\text{-DMophF})(\textit{o}\text{-DMophF}')$ (*o*-DMophF' = (*o*-methoxyphenyl)(*o*-oxyphenyl)formamidine anion) [2]. The nitrogen atoms of the *o*-DMophF[−] ligands in the quadruply bonded complexes, *cis*- $\text{Cr}_2(\text{O}_2\text{CCH}_3)_2(\textit{o}\text{-DMophF})_2$ and *trans*- $\text{Mo}_2(\text{O}_2\text{CCH}_3)_2(\textit{o}\text{-DMophF})_2$ [3], are bridged to the metal centers, while the oxygen atoms are not coordinated, **III**. No complex containing the neutral *o*-HDMophF ligand or its protonated form $\textit{o}\text{-H}_2\text{DMophF}^+$ has been reported. We report herein several mononuclear complexes of *o*-HDMophF ligands that coordinate to the metal centers in new bidentate and monodentate fashions, **IV** and **V**, respectively. The

* Corresponding author. Tel.: +88632653351; fax: +88632653399.
E-mail address: jdchen@cycu.edu.tw (J.-D. Chen).



Scheme 1. Bonding modes *o*-HDMophF ligand and its anion *o*-HDMophF⁻.

synthesis and structures of $\text{CuCl}_2 \cdot (\textit{o}\text{-HDMophF})$, $[\text{CoX}_4][\textit{o}\text{-H}_2\text{DMophF}]_2$ (X = Cl and Br) and $\text{MCl}_2 (\textit{o}\text{-HDMophF})_2$ (M = Cd, Ni, Mn and Pd) and the conformations of the neutral *o*-HDMophF and its protonated cation $\textit{o}\text{-H}_2\text{DMophF}^+$ form the subject of this report.

2. Experimental

2.1. General procedures

All manipulations were carried out under dry, oxygen-free nitrogen by using Schlenk techniques, unless otherwise noted. Solvents were dried and deoxygenated by refluxing over the appropriate reagents before use. *n*-Hexane and diethyl ether were purified by distillation from sodium/benzophenone, dichloromethane from P_2O_5 and acetonitrile from CaH_2 . The visible absorption spectra were recorded on a Hitachi U-2000 spectrophotometer. IR spectra were obtained from a Jasco FT/IR-460 plus spectrometer. Elemental analyses were obtained from a PE 2400 series II CHNS/O analyzer.

2.2. Materials

$\text{CoCl}_2 \cdot 6\text{H}_2\text{O}$, CoBr_2 , MnCl_2 , NiCl_2 and PdCl_2 were purchased from Strem Chemical Co. $\text{CuCl}_2 \cdot 2\text{H}_2\text{O}$ and $\text{CdCl}_2 \cdot \text{H}_2\text{O}$ were purchased from MERCK Co. The ligand *N,N'*-di(2-methoxyphenyl)formamidine (*o*-HDMophF) was prepared according to a previously reported procedure [1].

2.3. Preparations

2.3.1. $\text{CuCl}_2 \cdot (\textit{o}\text{-HDMophF})$

$\text{CuCl}_2 \cdot 2\text{H}_2\text{O}$ (0.17 g, 0.99 mmol) was added to a solution of *N,N'*-di(2-methoxyphenyl)formamidine (*o*-HDMophF) (0.25 g, 0.98 mmol) in 20 ml CH_2Cl_2 . The mixture was refluxed for 24 h and then allowed to cool down to room temperature to afford a brown solution and a dark brown solid. The solid was filtered out and *n*-hexane was added to induce precipitation. The precipitate was filtered and washed by ether (3×10 ml) and then dried under reduced pressure to give the dark brown product. Yield: 0.24 g (56%). UV-vis (CH_2Cl_2): 546 nm. *Anal.* Calc. for $\text{C}_{15}\text{H}_{16}\text{CuCl}_2\text{N}_2\text{O}_2$ (MW = 390.74), C, 46.11; H, 4.13; N, 7.17. Found: C, 46.13; H, 4.16; N, 7.23%. FT-IR (cm^{-1}) (KBr disk): 3197(b), 2963(s), 2345(w), 1685(s), 1638(s), 1594(s), 1524(m), 1508(w), 1459(s), 1340(m), 1286(w), 1259(s), 1175(w), 1113(s), 1021(s), 803(s), 750(s), 457(w), 419(w).

2.3.2. $[\text{CoCl}_4][\textit{o}\text{-H}_2\text{DMophF}]_2$

$\text{CoCl}_2 \cdot 6\text{H}_2\text{O}$ (0.24 g, 1.01 mmol) was added to a solution containing *o*-HDMophF (0.51 g, 1.99 mmol) in 20 ml CH_2Cl_2 . The mixture was then refluxed for 24 h and allowed to cool down to room temperature to afford a blue solution and a light blue solid. The solid was filtered out and then *n*-hexane was added to induce precipitation. The precipitate was filtered and washed by ether (3×10 ml) and then dried under vacuum to give the light blue product. Yield: 0.44 g (78.4%). UV-vis (CH_2Cl_2): 644 nm. *Anal.* Calc. for $\text{C}_{30}\text{H}_{34}\text{CoCl}_4\text{N}_4\text{O}_4$ (MW = 715.34), C, 50.37; H, 4.79; N, 7.83. Found: C, 49.93; H, 4.96; N, 7.70%. FT-IR (cm^{-1}) (KBr disk): 3447(b), 1718(w), 1685(s), 1655(s), 1637(w), 1560(m), 1541(s), 1524(w), 1508(m), 1459(s), 1259(s), 1113(m), 1023(s), 799(m), 750(s).

2.3.3. $[\text{CoBr}_4][\textit{o}\text{-H}_2\text{DMophF}]_2$

Procedures for **3** were similar to those for **2**. Yield: 0.36 g (40%). UV-vis (THF): 675 nm. *Anal.* Calc. for $\text{C}_{30}\text{H}_{34}\text{Br}_4\text{CoN}_4\text{O}_4$ (MW = 893.18), C, 40.34; H, 3.84; N, 6.27. Found: C, 40.47; H, 4.04; N, 5.86%. FT-IR (cm^{-1}) (KBr disk): 3448(b), 1716(w), 1685(s), 1654(s), 1633(w), 1562(m), 1541(s), 1520(w), 1509(m), 1458(s), 1257(s), 1116(m), 1025(s), 794(m), 753(s).

2.3.4. $\text{CdCl}_2(\textit{o}\text{-HDMophF})_2$

Procedures for **4** were similar to those for **2**. Yield: 0.41 g (60%). *Anal.* Calc. for $\text{C}_{30}\text{H}_{32}\text{CdCl}_2\text{N}_4\text{O}_4$ (MW = 695.92), C, 51.78; H, 4.62; N, 8.05. Found: C, 51.73; H, 4.68; N, 7.88%. UV-vis (CH_2Cl_2): 348 nm. FT-IR (cm^{-1}) (KBr disk): 3189(w), 2938(m), 1735(w), 1685(w), 1649(s), 1591(s), 1514(s), 1459(s), 1433(m), 1396(w), 1333(m), 1288(w), 1258(m), 1245(s), 1183(s), 1157(m), 1118(s), 1048(m), 1026(s), 790(w), 755(s), 669(w), 585(w), 485(w), 418(w).

Table 1
Crystal data for 1–7

Compound	1	2	3	4	5	6	7
Formula	CuC ₁₅ H ₁₆ Cl ₂ O ₂ N ₂	CoC ₃₀ H ₃₄ Cl ₄ O ₄ N ₄	C ₃₀ H ₃₄ Br ₄ CoN ₄ O ₄	CdC ₃₀ H ₃₂ Cl ₂ O ₄ N ₄	NiC ₃₀ H ₃₂ Cl ₂ O ₄ N ₄	MnC ₃₀ H ₃₂ Cl ₂ O ₄ N ₄	PdC ₃₀ H ₃₂ Cl ₂ O ₄ N ₄
Molecular weight	390.74	715.34	893.18	695.90	641.21	638.44	689.90
Crystal system	monoclinic	orthorhombic	orthorhombic	monoclinic	monoclinic	monoclinic	monoclinic
Space group	<i>P2₁/c</i>	<i>P2₁2₁2₁</i>	<i>P2₁2₁2₁</i>	<i>Cc</i>	<i>P2₁/c</i>	<i>P2₁/c</i>	<i>P2₁/c</i>
<i>a</i> (Å)	7.492(3)	9.6465(13)	9.7008(14)	26.625(5)	15.585(3)	15.8047(12)	7.3195(10)
<i>b</i> (Å)	10.497(4)	13.2075(14)	13.830(2)	38.421(8)	7.6594(16)	7.6909(10)	9.6643(10)
<i>c</i> (Å)	21.293(9)	26.888(2)	26.674(4)	15.974(3)	26.147(5)	26.080(4)	21.185(2)
β (°)	93.10(4)	90	90	108.938(3)	105.996(4)	105.628(10)	97.282(12)
<i>V</i> (Å ³)	1672.2(11)	3425.7(7)	3578.7(9)	15456(5)	3000.2(10)	3052.9(6)	1486.5(3)
<i>Z</i>	4	4	4	20	4	4	2
<i>D</i> _{calc} (g/cm ³)	1.552	1.387	1.658	1.495	1.422	1.389	1.541
<i>F</i> (000)	796	1476	1764	7080	1336	1324	704
μ (Mo K α) (mm ⁻¹)	1.632	0.852	0.648	0.920	0.867	0.648	0.846
Data collection instrument	Bruker AXS P4	Bruker AXS P4	Siemens CCD	Siemens CCD	Siemens CCD	Bruker AX4 P4	Bruker AXS P4
λ (Mo K α) (Å)	0.71073	0.71073	0.71073	0.71073	0.71073	0.71073	0.71073
Range (2 θ) for data collection (°)	3.84 \leq 2 θ \leq 50.00	4.32 \leq 2 θ \leq 49.98	4.24 \leq 2 θ \leq 50.08	4.24 \leq 2 θ \leq 50.04	4.78 \leq 2 θ \leq 50.12	3.60 \leq 2 θ \leq 50.00	3.88 \leq 2 θ \leq 50.00
Goodness-of-fit (GOF) ^c	1.083	1.012	1.009	1.200	1.000	1.026	1.010
Final <i>R</i> indices [<i>I</i> > 2 σ (<i>I</i>)] ^{a,b}	<i>R</i> ₁ = 0.0431, <i>wR</i> ₂ = 0.1217	<i>R</i> ₁ = 0.0358, <i>wR</i> ₂ = 0.0794	<i>R</i> ₁ = 0.0351, <i>wR</i> ₂ = 0.0576	<i>R</i> ₁ = 0.0493, <i>wR</i> ₂ = 0.0950	<i>R</i> ₁ = 0.0488, <i>wR</i> ₂ = 0.0464	<i>R</i> ₁ = 0.0312, <i>wR</i> ₂ = 0.0794	<i>R</i> ₁ = 0.0335, <i>wR</i> ₂ = 0.0686
<i>R</i> indices (all data)	<i>R</i> ₁ = 0.0556, <i>wR</i> ₂ = 0.1293	<i>R</i> ₁ = 0.0537, <i>wR</i> ₂ = 0.0881	<i>R</i> ₁ = 0.0680, <i>wR</i> ₂ = 0.0637	<i>R</i> ₁ = 0.1050, <i>wR</i> ₂ = 0.1240	<i>R</i> ₁ = 0.1199, <i>wR</i> ₂ = 0.0540	<i>R</i> ₁ = 0.0429, <i>wR</i> ₂ = 0.0862	<i>R</i> ₁ = 0.0611, <i>wR</i> ₂ = 0.0781
Largest difference peak and hole (e/Å ³)	0.441 and -0.479	0.240 and -0.181	0.392 and -0.421	0.554 and -0.608	0.326 and -0.267	0.196 and -0.238	0.439 and -0.514

$$^a R_1 = \frac{\sum ||F_o| - |F_c||}{\sum |F_o|}$$

$$^b wR_2 = \left[\frac{\sum w(F_o^2 - F_c^2)^2}{\sum w(F_o^2)^2} \right]^{1/2}, w = 1/[\sigma^2(F_o^2) + (ap)^2 + (bp)], p = [\max(F_o^2 \text{ or } 0) + 2(F_c^2)]/3. a = 0.0656, b = 0.9223, \mathbf{1}; a = 0.0461, b = 0.2958, \mathbf{2}; a = 0.0334, b = 0.0000, \mathbf{3}; a = 0.0278, b = 44.6029, \mathbf{4}; a = 0.0234, b = 0.0000, \mathbf{5}; a = 0.0422, b = 0.7088, \mathbf{6}; a = 0.0306, b = 0.7845, \mathbf{7}.$$

$$^c \text{GOF} = \left[\frac{\sum w(|F_o^2| - |F_c^2|)^2}{(N_{\text{observed}} - N_{\text{parameters}})} \right]^{1/2}.$$

2.3.5. $MnCl_2(o\text{-HDMophF})_2$

Procedures for **5** were similar to those for **2**. Yield: 0.52 g (82.3%). UV–vis (CH_2Cl_2): 425 nm. *Anal. Calc.* for $C_{30}H_{32}MnCl_2N_4O_4$ (MW = 638.45), C, 56.44; H, 5.05; N, 8.78. Found: C, 56.40; H, 5.07; N, 8.46%. FT-IR (cm^{-1}) (KBr disk): 3177(s), 3033(w), 2939(m), 1648(s), 1591(s), 1513(m), 1496(s), 1463(m), 1432(w), 1378(w), 1333(m), 1299(w), 1256(w), 1239(s), 1181(w), 1157(m), 1116(s), 1048(m), 1024(s), 924(m), 851(w), 831(w), 788(w), 753(s), 721(s), 625(m), 576(w).

2.3.6. $NiCl_2(o\text{-HDMophF})_2$

Procedures for **6** were similar to those for **2**. Yield: 0.37 g (57.6%). UV–vis (CH_2Cl_2): 362 nm. *Anal. Calc.* for $C_{30}H_{32}NiCl_2N_4O_4$ (MW = 642.20), C, 56.11; H, 5.02; N, 8.72. Found: C, 55.78; H, 4.98; N, 8.55%. FT-IR (cm^{-1}) (KBr disk): 3445(b), 3353(s), 3230(m), 2836(w), 1654(s), 1598(s), 1509(m), 1490(s), 1455(m), 1418(w), 1388(w), 1371(m), 1323(w), 1305(w), 1294(m), 1275(m), 1245(s), 1208(w), 1176(w), 1149(m), 1108(s), 1042(m), 1015(s), 951(m), 843(w), 787(w), 756(s), 598(m), 538(w), 507(w), 490(w), 467(w), 440(w).

2.3.7. $PdCl_2(o\text{-HDMophF})_2$

Procedures for **7** were similar to those for **2**. Yield: 0.46 g (77%). UV–vis (CH_2Cl_2): 502 nm. *Anal. Calc.* for $C_{30}H_{32}PdCl_2N_4O_4$ (MW = 689.93), C, 52.23; H, 4.67; N, 8.12. Found: C, 52.40; H, 4.66; N, 8.07%. FT-IR (cm^{-1}) (KBr disk): 3448(b), 3357(s), 3233(m), 2838(w), 1655(s), 1598(s), 1514(m), 1494(s), 1458(m), 1420(w), 1389(w), 1371(m), 1328(w), 1309(w), 1297(m), 1277(m), 1246(s), 1208(w), 1185(w), 1157(m), 1115(s), 1048(m), 1023(s), 955(m), 844(w), 789(w), 757(s), 598(m), 538(w), 507(w), 490(w), 467(w), 440(w).

2.4. X-ray crystallography

Single crystal X-ray diffraction data were collected at 22 °C using either a Bruker AXS P4 (complexes **1**, **2** and **6**) or a Siemens CCD diffractometer (complexes **2**, **4** and **5**), which were equipped with graphite-monochromated Mo K α (0.71073 Å) radiation. Data reduction was carried by standard methods with the use of well-established computational procedures [4].

A light yellow crystal of **1** was mounted on the top of a glass fiber with epoxy cement. Cell constants were derived from least-squares refinement of 40 reflections having $10.1 < 2\theta < 24.8$. The ω -scan data collection method was used to collect the data points at $3.84^\circ < 2\theta < 50.00^\circ$. The structure factors were obtained after Lorentz and polarization correction. An empirical absorption correction based on a series of ψ -scans was applied to the data. The positions of some of the heavier atoms, including the copper atom, were located by direct methods. The remaining atoms were found in a series of alternating difference Fourier maps and least-square

refinements [5]. The final residuals of the final refinement were $R_1 = 0.0459$, $wR_2 = 0.1233$. The crystallographic procedures for **2**, **6** and **7** were similar to those for **1**.

A yellow crystal of **3** was mounted on the top of a glass fiber with epoxy cement. The hemisphere data collection method was used to scan the data points at $4.24^\circ < 2\theta < 50.0^\circ$. The structure factors were obtained after Lorentz and polarization correction. An empirical absorption correction based on ‘multi-scan’ was applied to the data. The positions of some of the heavier atoms, including the Co atom, were located by direct methods. The remaining atoms were found in a series of alternating difference Fourier maps and least-square refinements [5]. The final residuals of the final refinement were $R_1 = 0.0351$, $wR_2 = 0.0673$. The crystallographic procedures for **4** and **5** were similar to those for **3**. For complex **4**, no solution can be obtained if $C2/c$ was used to solve the structure. The space group Cc was then selected to get the final structure.

For complexes **1**, **5**, **6** and **7**, all the hydrogen atoms, except the methyl hydrogen atom, H30A, H30B and H30C in **5**, were located in the difference electron density map and refined isotropically. The hydrogen atoms of complexes **2**, **3** and **4** and H30A, H30B and H30C in **5** were placed in geometrically calculated positions using the HADD program and refined using a riding model. Basic information pertaining to crystal parameters and structure refinement is summarized in Table 1.

3. Results and discussion

3.1. Synthesis

The reactions of *N,N'*-di(2-methoxyphenyl)formamidine (*o*-HDMophF) with $CuCl_2 \cdot 2H_2O$, $CoCl_2 \cdot 6H_2O$, $CoBr_2$, $CdCl_2 \cdot H_2O$, $MnCl_2$, $NiCl_2$ and $PdCl_2$ in refluxing CH_2Cl_2 afforded the complexes $CuCl_2 \cdot (o\text{-HDMophF})$, **1**, $[CoX_4][o\text{-H}_2\text{DMophF}]_2$ (X = Cl, **2**; Br, **3**) and $MCl_2(o\text{-HDMophF})_2$ (M = Cd, **4**; Ni, **5**; Mn, **6**; Pd, **7**), respectively. It is noted that although similar reaction conditions were used to prepare **1–7**, different types of products were obtained, presumably due to the different reactivity of the metal centers to *o*-HDMophF.

3.2. Structure of **1**

Yellow complex **1** was solved in the space group $P2_1/c$. Fig. 1 shows the ORTEP drawing of **1**, and the correct formulation for this complex is $CuCl_2 \cdot (o\text{-HDMophF})$. Selected bond distances and angles are listed in Table 2. The copper atom is bonded to two chlorine atoms to form a linear geometry. The two Cu–Cl distances are 2.1873(15) and 2.1752(15) Å and the Cl–Cu–Cl angle is 178.71(4)°. The packing diagram of complex **1** shows

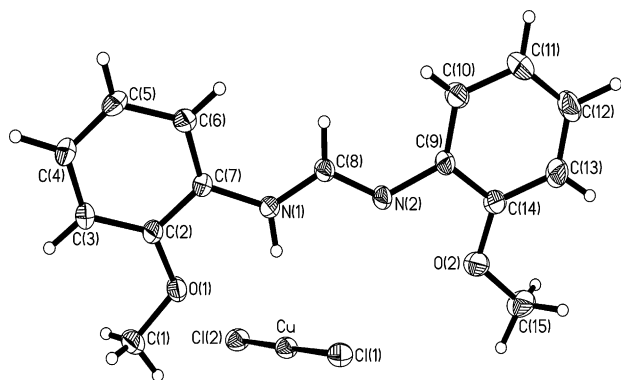


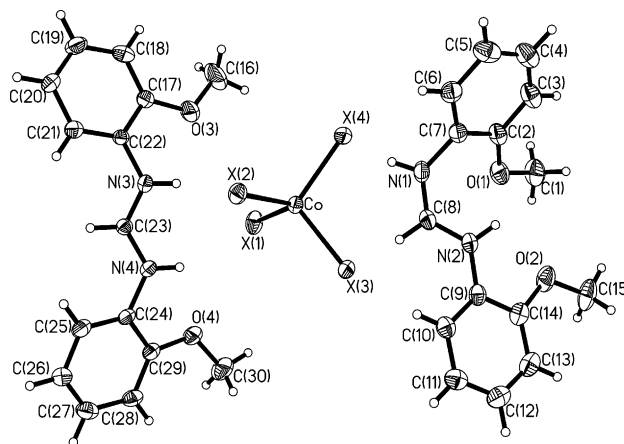
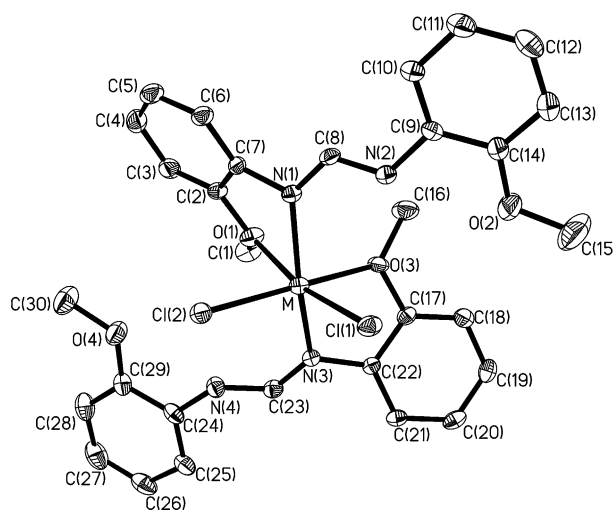
Fig. 1. An ORTEP diagram of complex 1.

that the metal units and *o*-HDMophF are interlinked through extensive N–H···Cl and C–H···Cl hydrogen bonds ($H\cdots Cl = 2.467\text{--}3.204\text{ \AA}$). Some weak Cu···O interactions (3.157 \AA) are also found.

3.3. Structures of 2 and 3

The structures of complexes 2 and 3 were solved in the space group $P2_12_12_1$, and a representative ORTEP drawing is shown in Fig. 2. Selected bond distances and angles are listed in Table 2. The Co atoms in 2 and 3 are bonded to four halide atoms, forming a distorted tetrahedral geometry. The Co–Cl lengths are in the range from 2.2560(12) to 2.2923(12) Å with the Cl–Co–Cl angles varying within the range from $106.34(5)^\circ$ to $113.23(5)^\circ$, while the Co–Br lengths are in the range from 2.3980(9) to 2.4171(9) Å with the Br–Co–Br angles varying within the range from $106.45(3)^\circ$ to $113.06(4)^\circ$. It is noted that two different conformations are observed for the *o*-H₂DMophF⁺ cations for each complex (vide infra).

The packing diagram of complex 2 and 3 shows that the molecules pack into layers of discrete CoX_4^{2-} ($X = Cl, 2$ and $Br, 3$) anions which are separated by layers of the *o*-H₂DMophF⁺ cations. The ions interact

Fig. 2. A representative ORTEP drawing of complexes 2 ($X = Cl$) and 3 ($X = Br$).Fig. 3. A representative ORTEP drawing of complexes 4 ($M = Cd$), 5 ($M = Ni$) and 6 ($M = Mn$), showing a Δ configuration.

through extensive N–H···X and C–H···X hydrogen bonds ($H\cdots Cl = 2.521\text{--}2.903\text{ \AA}$, $\angle N\text{--}H\cdots Cl$ and $\angle C\text{--}H\cdots Cl = 147.5\text{--}175.3^\circ$; $H\cdots Br = 2.527\text{--}3.037\text{ \AA}$,

Table 2
Selected bond distances (Å) and angles ($^\circ$) for 1–3

1		2		3	
<i>Bond distances</i>					
Cu(1)–Cl(2)	2.1752(15)	Co–Cl(2)	2.2560(12)	Co–Br(1)	2.3980(9)
Cu(1)–Cl(1)	2.1873(15)	Co–Cl(3)	2.2733(12)	Co–Br(3)	2.4170(10)
		Co–Cl(1)	2.2772(13)	Co–Br(4)	2.4037(9)
		Co–Cl(4)	2.2923(12)	Co–Br(2)	2.4171(9)
<i>Bond angles</i>					
Cl(2)–Cu(1)–Cl(1)	178.71(4)	Cl(2)–Co–Cl(3)	108.49(5)	Br(1)–Co–Br(4)	106.45(3)
		Cl(3)–Co–Cl(1)	111.11(6)	Br(4)–Co–Br(3)	111.07(4)
		Cl(3)–Co–Cl(4)	106.79(4)	Br(4)–Co–Br(2)	113.06(4)
		Cl(2)–Co–Cl(1)	106.34(5)	Br(1)–Co–Br(3)	111.04(4)
		Cl(2)–Co–Cl(4)	110.83(5)	Br(1)–Co–Br(2)	107.60(4)
		Cl(1)–Co–Cl(4)	113.23(5)	Br(3)–Co–Br(2)	107.59(3)

Table 3
Selected bond distances (Å) and angles (°) for **4**

Cd(1)		Cd(2)		Cd(3)		Cd(4)		Cd(5)	
<i>Bond distances</i>									
Cd(1)–N(3)	2.299(9)	Cd(2)–N(7)	2.319(9)	Cd(3)–N(11)	2.298(10)	Cd(4)–N(13)	2.315(11)	Cd(5)–N(17)	2.324(12)
Cd(1)–N(1)	2.355(9)	Cd(2)–N(5)	2.351(10)	Cd(3)–N(9)	2.344(12)	Cd(4)–N(15)	2.319(11)	Cd(5)–N(19)	2.334(11)
Cd(1)–Cl(1)	2.493(4)	Cd(2)–Cl(4)	2.472(3)	Cd(3)–Cl(6)	2.480(4)	Cd(4)–Cl(7)	2.459(4)	Cd(5)–Cl(10)	2.491(5)
Cd(1)–Cl(2)	2.493(4)	Cd(2)–Cl(3)	2.482(3)	Cd(3)–Cl(5)	2.497(3)	Cd(4)–Cl(8)	2.474(5)	Cd(5)–Cl(9)	2.502(5)
Cd(1)–O(1)	2.551(8)	Cd(2)–O(5)	2.527(9)	Cd(3)–O(11)	2.560(9)	Cd(4)–O(15)	2.562(11)	Cd(5)–O(17)	2.525(10)
Cd(1)–O(3)	2.601(8)	Cd(2)–O(7)	2.620(8)	Cd(3)–O(9)	2.585(9)	Cd(4)–O(13)	2.578(10)	Cd(5)–O(19)	2.574(10)
<i>Bond angles</i>									
N(3)–Cd(1)–N(1)	147.0(3)	N(7)–Cd(2)–N(5)	146.3(3)	N(11)–Cd(3)–N(9)	147.2(4)	N(13)–Cd(4)–N(15)	146.8(4)	N(17)–Cd(5)–N(19)	147.6(4)
N(3)–Cd(1)–Cl(1)	102.0(2)	N(7)–Cd(2)–Cl(4)	98.4(2)	N(11)–Cd(3)–Cl(6)	95.2(3)	N(13)–Cd(4)–Cl(7)	97.4(3)	N(17)–Cd(5)–Cl(10)	99.2(3)
N(1)–Cd(1)–Cl(1)	94.7(2)	N(5)–Cd(2)–Cl(4)	100.1(2)	N(9)–Cd(3)–Cl(6)	100.2(3)	N(15)–Cd(4)–Cl(7)	101.4(3)	N(19)–Cd(5)–Cl(10)	95.4(3)
N(3)–Cd(1)–Cl(2)	97.7(2)	N(7)–Cd(2)–Cl(3)	101.3(2)	N(11)–Cd(3)–Cl(5)	100.0(2)	N(13)–Cd(4)–Cl(8)	100.3(3)	N(17)–Cd(5)–Cl(9)	98.2(3)
N(1)–Cd(1)–Cl(2)	100.0(2)	N(5)–Cd(2)–Cl(3)	96.2(2)	N(9)–Cd(3)–Cl(5)	98.8(3)	N(15)–Cd(4)–Cl(8)	95.8(3)	N(19)–Cd(5)–Cl(9)	100.9(3)
Cl(1)–Cd(1)–Cl(2)	116.3(1)	Cl(4)–Cd(2)–Cl(3)	114.6(1)	Cl(6)–Cd(3)–Cl(5)	116.5(1)	Cl(7)–Cd(4)–Cl(8)	115.7(2)	Cl(10)–Cd(5)–Cl(9)	116.6(2)
N(3)–Cd(1)–O(1)	88.0(3)	N(7)–Cd(2)–O(5)	86.1(3)	N(11)–Cd(3)–O(11)	65.3(3)	N(13)–Cd(4)–O(15)	87.7(3)	N(17)–Cd(5)–O(17)	66.2(4)
N(1)–Cd(1)–O(1)	64.2(3)	N(5)–Cd(2)–O(5)	64.9(3)	N(9)–Cd(3)–O(11)	86.0(3)	N(15)–Cd(4)–O(15)	64.2(4)	N(19)–Cd(5)–O(17)	90.1(4)
Cl(1)–Cd(1)–O(1)	88.1(2)	Cl(4)–Cd(2)–O(5)	152.5(3)	Cl(6)–Cd(3)–O(11)	89.2(2)	Cl(7)–Cd(4)–O(15)	155.0(3)	Cl(10)–Cd(5)–O(17)	157.3(3)
Cl(2)–Cd(1)–O(1)	152.8(2)	Cl(3)–Cd(2)–O(5)	90.7(3)	Cl(5)–Cd(3)–O(11)	152.1(2)	Cl(8)–Cd(4)–O(15)	87.1(2)	Cl(9)–Cd(5)–O(17)	83.7(3)
N(3)–Cd(1)–O(3)	63.9(3)	N(7)–Cd(2)–O(7)	63.7(3)	N(11)–Cd(3)–O(9)	91.0(3)	N(13)–Cd(4)–O(13)	65.2(4)	N(17)–Cd(5)–O(19)	87.4(4)
N(1)–Cd(1)–O(3)	89.8(3)	N(5)–Cd(2)–O(7)	89.8(3)	N(9)–Cd(3)–O(9)	65.0(4)	N(15)–Cd(4)–O(13)	88.8(3)	N(19)–Cd(5)–O(19)	64.3(3)
Cl(1)–Cd(1)–O(3)	156.0(2)	Cl(4)–Cd(2)–O(7)	85.8(2)	Cl(6)–Cd(3)–O(9)	158.0(2)	Cl(7)–Cd(4)–O(13)	86.5(3)	Cl(10)–Cd(5)–O(19)	88.2(2)
Cl(2)–Cd(1)–O(3)	86.0(2)	Cl(3)–Cd(2)–O(7)	157.1(2)	Cl(5)–Cd(3)–O(9)	83.0(2)	Cl(8)–Cd(4)–O(13)	155.7(3)	Cl(9)–Cd(5)–O(19)	153.0(2)
O(1)–Cd(1)–O(3)	72.7(3)	O(5)–Cd(2)–O(7)	71.9(3)	O(11)–Cd(3)–O(9)	74.2(3)	O(15)–Cd(4)–O(13)	73.4(3)	O(17)–Cd(5)–O(19)	74.4(3)

Table 4
Selected bond distances (Å) and angles (°) for 5–7

5		6		7	
<i>Bond distances</i>					
Ni–N(1)	2.078(3)	Mn–N(3)	2.2492(13)	Pd–N(1)	2.019(3)
Ni–N(3)	2.080(3)	Mn–N(2)	2.2550(13)	Pd–Cl	2.2986(10)
Ni–O(1)	2.211(2)	Mn–O(2)	2.3858(13)		
Ni–O(3)	2.218(2)	Mn–O(3)	2.4097(13)		
Ni–Cl(1)	2.3501(11)	Mn–Cl(1)	2.4157(6)		
Ni–Cl(2)	2.3528(11)	Mn–Cl(2)	2.4089(6)		
<i>Bond angles</i>					
N(1)–Ni–N(3)	160.74(10)	N(3)–Mn–O(2)	89.07(5)	N(1)–Pd–N(1A)	180.00(14)
N(1)–Ni–O(1)	73.57(10)	N(3)–Mn–N(2)	151.65(6)	N(1)–Pd–Cl(A)	90.90(9)
N(3)–Ni–O(1)	91.20(10)	N(3)–Mn–Cl(2)	97.38(4)	Cl(A)–Pd–Cl	180.00(7)
N(1)–Ni–O(3)	92.09(9)	N(2)–Mn–O(2)	67.89(5)	N(1)–Pd–Cl	89.10(9)
N(3)–Ni–O(3)	73.97(10)	O(2)–Mn–Cl(2)	159.76(4)	N(1A)–Pd–Cl	90.90(9)
O(1)–Ni–O(3)	82.78(9)	N(2)–Mn–Cl(2)	99.48(4)		
N(1)–Ni–Cl(1)	99.34(8)	N(2)–Mn–O(3)	89.70(5)		
N(3)–Ni–Cl(1)	93.64(8)	N(3)–Mn–O(3)	68.12(5)		
O(1)–Ni–Cl(1)	168.54(6)	Cl(2)–Mn–O(3)	88.40(4)		
O(3)–Ni–Cl(1)	88.58(7)	O(2)–Mn–O(3)	76.19(5)		
N(1)–Ni–Cl(2)	92.06(8)	N(2)–Mn–Cl(1)	95.71(4)		
N(3)–Ni–Cl(2)	99.79(8)	N(3)–Mn–Cl(1)	100.21(4)		
O(1)–Ni–Cl(2)	89.85(7)	Cl(2)–Mn–Cl(1)	108.80(2)		
O(3)–Ni–Cl(2)	170.17(7)	O(2)–Mn–Cl(1)	88.72(4)		
Cl(1)–Ni–Cl(2)	99.53(4)	O(3)–Mn–Cl(1)	160.74(4)		

$\angle C-H \cdots Br$ and $\angle N-H \cdots Br = 122.0$ – 171.2°). The distance of the π – π stacking interactions is 4.002 Å.

3.4. Structures of 4–6

Pale crystals of **4** conform to the space group *Cc* with twenty molecules in a unit cell. Five independent $CdCl_2(o\text{-HDMophF})_2$ molecules were found in each asymmetric unit of **4**. Light yellow crystals of **5** and colorless crystals of **6** all conform to the space group *P2₁/c* with four molecules in a unit cell. Fig. 3 shows the representative ORTEP drawing for the complexes **4**–**6**. Selected bond lengths and angles for **4**–**6** are listed in Tables 3 and 4, respectively. It is seen from Fig. 3 that the metal atoms are bonded to two *cis* chloride atoms, two *trans* amine nitrogen atoms and two *cis* methoxy oxygen atoms. The *o*-HDMophF ligands chelate the center metal atoms through the amine nitrogen atom and the methoxy oxygen atom to form five-membered rings. The neutral *o*-HDMophF ligands in complexes **4**–**6** are thus coordinated to the metal centers in a new bidentate bonding mode, as shown in IV, Scheme 1. The metal centers, which adopt a distorted octahedral coordination geometry, have bond angles that significantly deviate from 90° or 180° , presumably due to the chelation of the bidentate *o*-HDMophF ligands. The bis-chelate complexes are all chiral, showing either Δ or Λ configuration, and have approximate C_2 symmetries. As seen in Table 3, the five independent molecules show subtle differences in the bond distances and angles. It is also noted that in complexes **4**–**6** the M–O distances

are all significantly longer than the M–N distances. The molecules interact through extensive $C-H \cdots Cl$ hydrogen bonds by means of interactions among the chloride atoms and the $C-H$ hydrogen atoms of the bidentate *o*-HDMophF ligand. The $C-H \cdots Cl$ distances are in the range from 2.705 to 2.879 Å.

3.5. Structure of 7

Yellow crystals of **7** conform to the space group *P2₁/c* with two molecules in the unit cell. Fig. 4 shows the

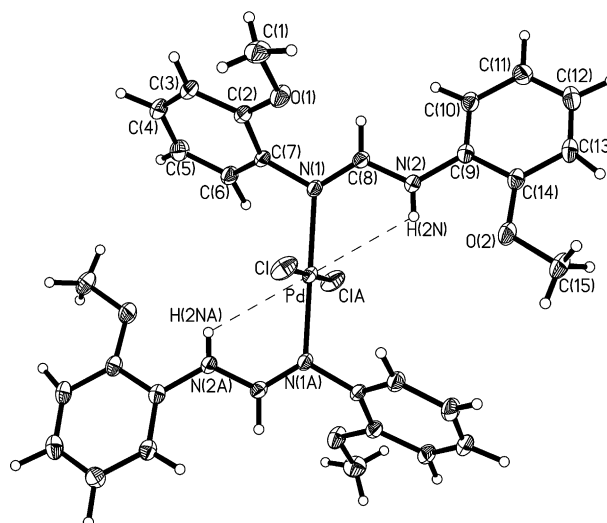


Fig. 4. An ORTEP drawing of complex **7**.

ORTEP drawing for complex **7** and some selected bond distances and angles of interest are given in Table 4. The palladium atom which adopts a distorted square planar coordination geometry is bonded to two *trans* chloride atoms (Pd–Cl = 2.2986(10) Å) and two *trans* amine nitrogen atoms (Pd–N(1) = 2.019(3) Å). In marked contrast to the bonding mode adopted in complexes **4–6**, the neutral *o*-HDMophF ligands are coordinated to the Pd atom through only one of the two nitrogen atoms. The oxygen atoms are not coordinated. The neutral *o*-HDMophF ligands in complex **7** are thus coordinated to the metal centers in a new monodentate bonding mode, as shown in V, Scheme 1. It is also noted that two short N–H···Pd distances (Pd···H = 2.794 Å, ∠Pd···H–N = 116.0°) which are *trans* to each other are observed.

The molecules interact through extensive C–H···Cl hydrogen bonds by means of interactions among the

chloride atoms and the C–H hydrogen atoms of the monodentate *o*-HDMophF ligand. The C–H···Cl distance is 2.794 Å and the C–H···Cl angle is 160.9°.

3.5.1. Conformation of the neutral *o*-HDMophF and the cation *o*-H₂DMophF⁺

The neutral *o*-HDMophF or *o*-H₂DMophF⁺ cation in each complex is not flat, but twisted around the C–N bonds. Table 5 lists the dihedral angles between the two phenyl rings of the neutral *o*-HDMophF or *o*-H₂DMophF⁺ cation in each complex, as well as the torsional angles used to define their conformations (vide infra, Table 6). It is seen from Table 5 that complex **7** shows the largest dihedral angle. A conformational descriptor for anionic diarylformamidate bearing an *m*-alkoxy substituent has been proposed by Ren and co-authors [6]. Based on their proposition, three stable

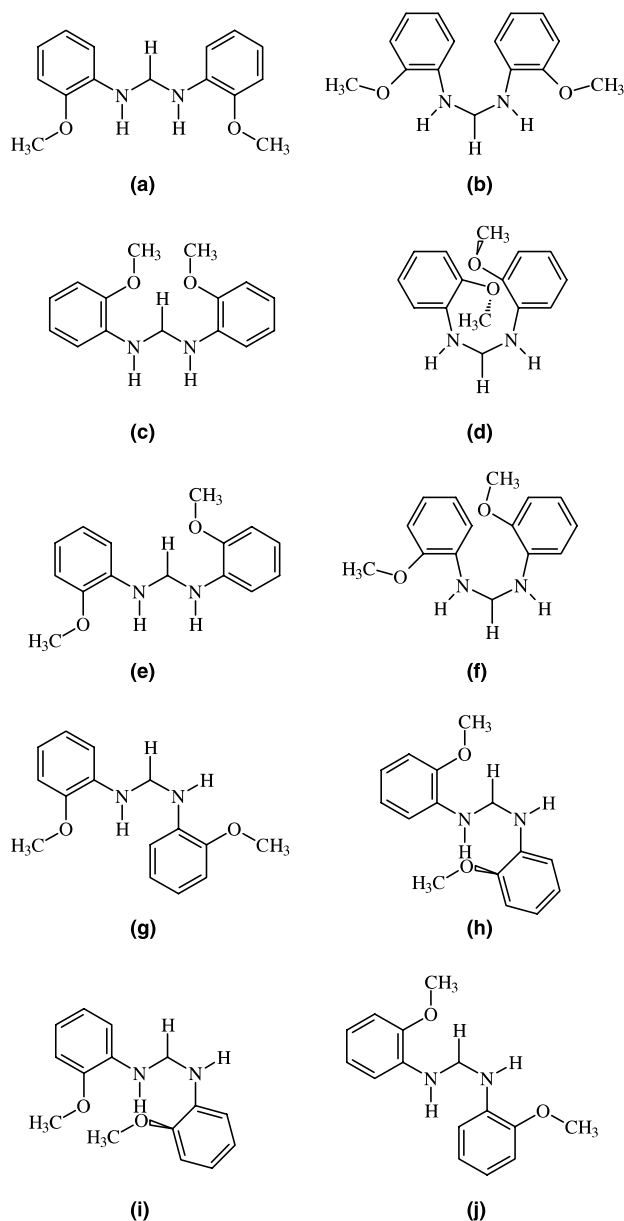
Table 5
Dihedral angles (°) and torsion angles (°) for *o*-HDMophF and *o*-H₂DMophF⁺ in complexes **1–7**

Complex	Dihedral angle (°)		Torsion angle (°)					
1	7.9		169.9					173.6
2	27.2	43.7	51.2	156.0	152.5	160.2		
3	24.5	40.4	48.3	154.3	154.9	162.1		
4, Cd(1)	39.5	41.6	141.6	143.7	141.7	139.6		
4, Cd(2)	41.7	42.2	141.7	142.7	140.6	139.5		
4, Cd(3)	38.4	45.9	145.4	144.0	143.5	145.7		
4, Cd(4)	37.1	42.1	144.4	142.3	143.0	139.6		
4, Cd(5)	39.5	44.5	144.8	146.1	140.3	145.6		
5	30.8	40.2	147.2	155.4	144.8	143.1		
6	33.7	40.0	151.7	144.2	143.8	141.9		
7	74.2		55.4					163.4

Table 6
The conformations of *o*-HDMophF, *o*-DMophF[−] and *o*-H₂DMophF⁺ in transition metal complexes

Complex	Bonding modes	Conformation	Reference
Ag ₂ (<i>o</i> -DMophF) ₂	I	<i>s-trans, s-trans</i>	[1]
<i>trans</i> -Ru ₂ (O ₂ CCH ₃) ₂ (<i>o</i> -DMophF)(<i>o</i> -DMophF')	II	<i>s-cis, s-trans</i>	[2]
<i>cis</i> -Ru ₂ (O ₂ CCH ₃) ₂ (<i>o</i> -DMophF) ₂ (<i>o</i> -DMophF')	III	<i>s-cis, s-trans</i>	[2]
Cr ₂ (<i>o</i> -DMophF) ₄	III	<i>s-cis, s-cis; s-cis, s-trans</i>	[9]
<i>cis</i> -Cr ₂ (O ₂ CCH ₃) ₂ (<i>o</i> -DMophF) ₂	III	<i>s-cis, s-trans</i>	[3a]
Mo ₂ (O ₂ CCH ₃) ₃ (<i>o</i> -DMophF)	III	<i>s-trans, s-trans</i>	[3b]
<i>trans</i> -Mo ₂ (O ₂ CCF ₃) ₂ (<i>o</i> -DMophF) ₂	III	<i>s-cis, s-trans</i>	[3b]
<i>trans</i> -Mo ₂ (O ₂ CPr ⁿ) ₂ (<i>o</i> -DMophF) ₂	III	<i>s-cis, s-trans</i>	[3b]
<i>trans</i> -Mo ₂ (O ₂ CCH ₃) ₂ (<i>o</i> -DMophF) ₂	III	<i>s-cis, s-trans</i>	[3b]
Mo ₂ (O ₂ CCH ₃)(<i>o</i> -DMophF)Cl ₂ (PMe ₃) ₂	III	<i>s-cis, s-trans</i>	[3b]
<i>trans</i> -Mo ₂ (O ₂ CCH ₃)(DpyF)(<i>o</i> -DMophF) ₂	III	<i>s-cis, s-trans</i>	[10]
<i>trans</i> -Mo ₂ (O ₂ CCH ₃)(DpmF)(<i>o</i> -DMophF) ₂	III	<i>s-cis, s-trans</i>	[10]
<i>trans</i> -Mo ₂ (O ₂ CCH ₃)(DMepyF) ₂ (<i>o</i> -DMophF)	III	<i>s-cis, s-cis</i>	[10]
<i>trans</i> -Mo ₂ (DMepyF) ₂ (<i>o</i> -DMophF) ₂	III	<i>s-cis, s-cis</i>	[10]
1		<i>s-trans-anti-s-trans</i>	this work
2		<i>s-cis-syn-anti-s-trans</i> <i>s-trans-anti-anti-s-trans</i>	this work
3		<i>s-cis-syn-anti-s-trans</i> <i>s-trans-anti-anti-s-trans</i>	this work
4	IV	<i>s-trans-anti-s-trans</i>	this work
5	IV	<i>s-trans-anti-s-trans</i>	this work
6	IV	<i>s-trans-anti-s-trans</i>	this work
7	V	<i>s-cis-anti-s-trans</i>	this work

conformations exist for diarylformamidines which are defined as (a) *s-cis,s-cis-* (*s-cis/s-trans-* are defined between N–C (methine) bond and the ring C–C bond prioritized by the OR group), (b) *s-cis-s-trans-*, and (c) *s-trans-s-trans-*, respectively. To describe the conformations for the neutral *N,N'*-di(2-pyridyl)formamidines (HDpyF) and *N,N'*-di(6-methyl-2-pyridyl)formamidines (HDMepyF) ligands, where the amine hydrogen atoms are retained, we have modified this descriptor and show eight possible conformations for the neutral dipyridylformamidines ligands [7]. These eight conformations are: (a)



Scheme 2. Possible conformation for the cationic *o*-H₂DMophF⁺ ligands. (a) *s-trans-anti-anti-s-trans*; (b) *s-trans-syn-syn-s-trans*; (c) *s-cis-anti-anti-s-cis*; (d) *s-cis-syn-syn-s-cis*; (e) *s-trans-anti-anti-s-cis*; (f) *s-trans-syn-syn-s-cis*; (g) *s-trans-trans-syn-s-trans*; (h) *s-cis-anti-syn-s-cis*; (i) *s-trans-anti-syn-s-cis*; and (j) *s-cis-anti-syn-trans*.

s-trans-anti-s-trans, (b) *s-trans-anti-s-cis*, (c) *s-cis-anti-s-trans*, (d) *s-cis-anti-s-cis*, (e) *s-trans-syn-s-trans*, (f) *s-trans-syn-s-cis*, (g) *s-cis-syn-s-trans*, and (h) *s-cis-syn-s-cis*, where *syn* and *anti* indicate the relative positions of the methine and amine hydrogen atoms, respectively. Based on this descriptor, the conformations of the neutral *o*-HDMophF in complexes **1**, **4**, **5** and **6** are assigned as *s-trans-anti-s-trans* while that in complex **7** is *s-cis-anti-s-trans*.

To describe the conformation for the *o*-H₂DMophF⁺ cations in complexes **2** and **3** which contains two amine hydrogen atoms, one more *syn* or *anti* should be added to describe the relative position of the amine hydrogen atoms. As shown in Scheme 2, 10 possible conformations can be drawn for the *o*-H₂DMophF⁺ cation. Based on this new descriptor, the conformations of the two *o*-H₂DMophF⁺ cations in complexes **2** and **3** are assigned as *s-cis-syn-anti-s-trans* and *s-trans-anti-anti-s-trans*. Table 6 lists the conformations of the neutral *o*-HDMophF, anionic *o*-DMophF[−] and cationic *o*-H₂DMophF⁺ adopted in the metal complexes reported so far. For comparison, it is noted that the conformation of the cationic H₂DMepyF⁺ ligands in the complexes *trans*-[Mo₂(H₂DMepyF)₂(CH₃CN)₄](*ax*-CH₃CN)₂(BF₄)₆ · 2CH₃CN and *trans*-[Mo₂(H₂DMepyF)₂(CH₃CN)₄](*ax*-BF₄)₂(BF₄)₄ · 2CH₃CN are similar to those in the anionic diarylformamidines ligands since the amine hydrogen atoms have been removed and these cationic ligands were assigned the *s-cis*, *s-cis* conformation [8].

4. Conclusions

The synthesis and structures of seven complexes containing neutral *o*-HDMophF or its cation *o*-H₂DMophF⁺ have been successfully accomplished. The *o*-HDMophF ligands in complexes **4–6** and **7** are coordinated to the metal centers in new bidentate and monodentate bonding modes, respectively. All of them show supramolecular structures in the solid state by various types of weak interactions, including C–H···X and N–H···X (X = Cl or Br) hydrogen bondings and π–π stacking interactions.

The neutral *o*-HDMophF ligands in complexes **1**, **4**, **5** and **6** adopt the *s-trans-anti-s-trans* conformation while that in complex **7** adopts the *s-cis-anti-s-trans* conformation. The *o*-H₂DMophF⁺ cations in **2** and **3** adopt the new *s-cis-syn-anti-s-trans*- and *s-trans-anti-anti-s-trans*-conformations.

Acknowledgements

We are grateful to the National Science Council of the Republic of China for support.

Appendix A. Supplementary data

Crystallographic data (CIF files) for the structures **1–7** have been deposited with the Cambridge Crystallographic Data Centre, CCDC Nos. 238743–238749. Copies of this information may be obtained free of charge from The Director, CCDC, 12 Union Road, Cambridge CB2 1EZ, UK (fax: +44 1223 336 033; e-mail: deposit@ccdc.cam.ac.uk or www: <http://www.ccdc.cam.ac.uk>). The packing diagrams for complexes **1–7** and the ORTEP diagrams for the five independent molecules of complex **4** are also available (9 pages). Supplementary data associated with this article can be found, in the on-line version at [doi:10.1016/j.poly.2004.12.012](https://doi.org/10.1016/j.poly.2004.12.012).

References

- [1] (a) S.J. Archibald, N.W. Alcock, D.H. Busch, D.R. Whitcomb, *Inorg. Chem.* 38 (1999) 5571; (b) T. Ren, C. Lin, P. Amalberti, D. Macikenas, J.D. Protasiewicz, J.C. Baum, T.L. Gibson, *Inorg. Chem. Commun.* 1 (1998) 23.
- [2] T. Ren, V. DeSilva, G. Zou, C. Lin, L.M. Daniels, C.F. Campana, J.C. Alvarez, *Inorg. Chem. Commun.* 2 (1999) 301.
- [3] (a) F.A. Cotton, L.M. Daniels, C.A. Murillo, P. Schooler, *J. Chem. Soc., Dalton Trans.* (2000) 2001; (b) Y.-Y. Wu, J.-D. Chen, L.-S. Liou, J.-C. Wang, *Inorg. Chim. Acta* 336 (2002) 71.
- [4] (a) SMART/SAINT/ASTRO, Release, 4.03, Siemens Energy and Automation, Inc., Madison, WI, 1995; (b) XSCANS, Release, 2.1, Siemens Energy and Automation, Inc., Madison, WI, 1995.
- [5] SHELXTL-5.10. Bruker Analytical X-ray Instruments Inc., Karlsruhe, Germany, 1997.
- [6] S. Radak, Y. Ni, G. Xu, K.L. Shaffer, T. Ren, *Inorg. Chim. Acta* 321 (2001) 200.
- [7] H.-C. Liang, Y.-Y. Wu, F.-C. Chang, P.-Y. Yang, J.-D. Chen, J.-C. Wang, *J. Organomet. Chem.* 669 (2003) 182.
- [8] H.-Y. Weng, Y.-Y. Wu, C.-P. Wu, J.-D. Chen, *Inorg. Chim. Acta* 356 (2004) 1369.
- [9] F.A. Cotton, L.M. Daniels, C.A. Murillo, P. Schooler, *J. Chem. Soc., Dalton Trans.* (2000) 2007.
- [10] Y.-Y. Wu, T.-C. Kao, J.-D. Chen, C.-H. Hung, *Inorg. Chim. Acta* 357 (2004) 1002.